



Lawrence Berkeley Laboratory

UNIVERSITY OF CALIFORNIA

Accelerator & Fusion Research Division

RECEIVED
LAWRENCE
BERKELEY LABORATORY

JUN 9 1988

Submitted to Review of Scientific Instruments

LIBRARY AND
DOCUMENTS SECTION

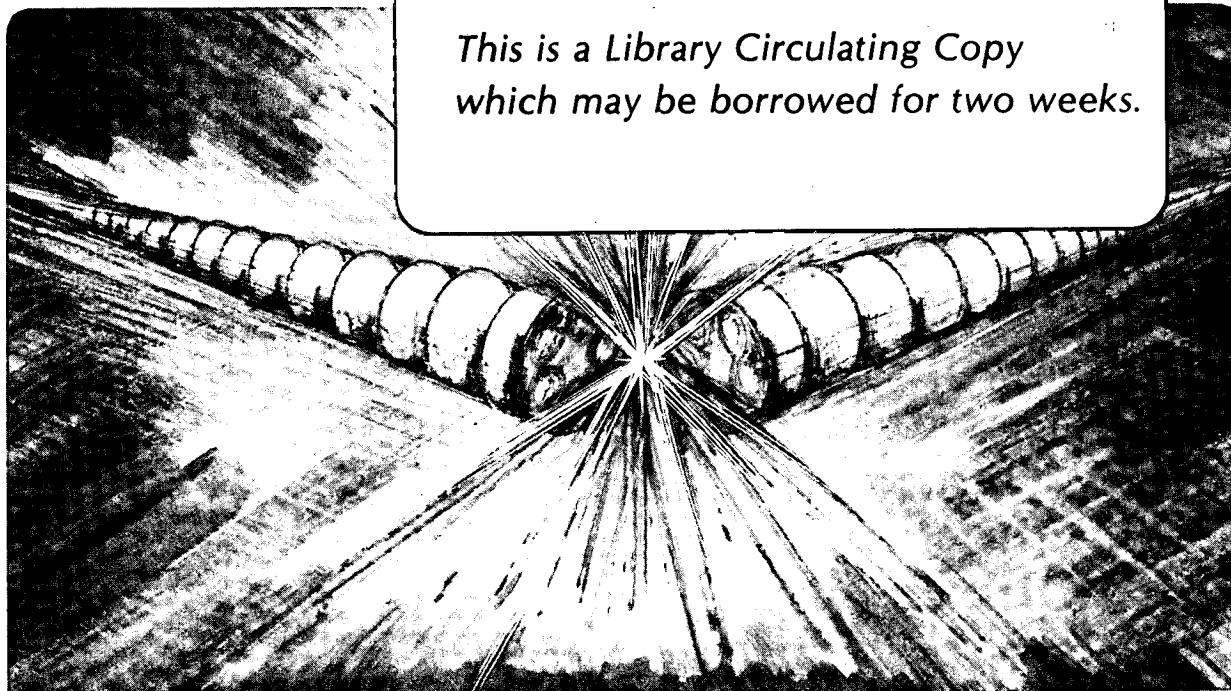
A VUV Laser-Absorption-Spectrometer System for Measurement of H^0 Density and Temperature in a Plasma

G.C. Stutzin, A.T. Young, A.S. Schlachter, J.W. Stearns,
K.N. Leung, W.B. Kunkel, G.T. Worth, and R.R. Stevens

February 1988

TWO-WEEK LOAN COPY

*This is a Library Circulating Copy
which may be borrowed for two weeks.*



LBL-24860
e.2

DISCLAIMER

This document was prepared as an account of work sponsored by the United States Government. While this document is believed to contain correct information, neither the United States Government nor any agency thereof, nor the Regents of the University of California, nor any of their employees, makes any warranty, express or implied, or assumes any legal responsibility for the accuracy, completeness, or usefulness of any information, apparatus, product, or process disclosed, or represents that its use would not infringe privately owned rights. Reference herein to any specific commercial product, process, or service by its trade name, trademark, manufacturer, or otherwise, does not necessarily constitute or imply its endorsement, recommendation, or favoring by the United States Government or any agency thereof, or the Regents of the University of California. The views and opinions of authors expressed herein do not necessarily state or reflect those of the United States Government or any agency thereof or the Regents of the University of California.

**A VUV LASER-ABSORPTION-SPECTROMETER SYSTEM
FOR MEASUREMENT OF H⁰ DENSITY AND TEMPERATURE
IN A PLASMA***

G. C. STUTZIN, a) A. T. YOUNG, A. S. SCHLACHTER, J. W. STEARNS,
K. N. LEUNG, and W. B. KUNKEL a)

Lawrence Berkeley Laboratory

University of California

Berkeley, CA 94720

and

G. T. WORTH and R. R. STEVENS

Los Alamos National Laboratory

Los Alamos, New Mexico 87545

February 1988

a) also associated with Department of Physics, University of California, Berkeley,
CA 94720

* Supported by Los Alamos National Laboratory, Air Force Office for Scientific
Research, and U. S. D.O.E. under contract No. DE-AC03-76SF00098.

SUBMITTED TO REVIEW OF SCIENTIFIC INSTRUMENTS

**A VUV Laser-Absorption-Spectrometer System for Measurement of
H⁰ Density and Temperature in a Plasma**

G. C. STUTZIN, ^{a)} A. T. YOUNG, A. S. SCHLACHTER, J. W. STEARNS,
K. N. LEUNG, and W. B. KUNKEL ^{a)}

Lawrence Berkeley Laboratory

University of California

Berkeley, CA 94720

and

G. T. WORTH and R. R. STEVENS

Los Alamos National Laboratory

Los Alamos, New Mexico 87545

ABSTRACT

A system to determine the density and temperature of ground-state hydrogen atoms in a hydrogen plasma by measurement of the absorption of Lyman-beta or Lyman-gamma radiation is described. The Lyman-series radiation is generated by resonant four-wave sum-frequency mixing in mercury vapor. A wide range of hydrogen atom densities can be measured by employing these two transitions. A sample measurement on an H⁺ ion-source discharge is presented. Extensions to Lyman-alpha and other vacuum ultraviolet wavelengths are discussed.

INTRODUCTION

Measurement of the H-atom density in hydrogen plasmas is of interest for understanding the process of H^- production. In volume-production negative ion-sources, H^- is believed to be created by a two-step process in which fast electrons (>40 eV) first produce vibrationally excited hydrogen molecules, $H_2(v>0)$, which subsequently capture slow electrons (~ 1 eV) and dissociate, forming H^0 and H^- .^{1,2} The rate of destruction of H^- by the inverse reaction clearly depends on the H^0 density. Collisions with H-atoms can also serve to vibrationally relax $H_2(v)$,³ and recent evidence indicates that atoms can recombine on a surface to form $H_2(v)$.⁴ In the Dudnikov-type Penning source,⁵ it is speculated that cold H^- ions are formed by charge exchange between fast H^- ions and low energy H^0 atoms near the extraction region.⁶ To investigate the dependence of extracted negative ion current upon H-atom density, we have developed a method to measure this density in a plasma directly.

Several methods can be used to determine atom density. Emission spectroscopy on Balmer lines has been used to measure the ratio of atomic to molecular hydrogen in a ion-source discharge,⁷ and to measure the relative variation in atom density in a Z-discharge plasma.⁸ Modeling was required to interpret the measured data in both experiments. Resonance fluorescence is a well known technique and has been used recently to measure the density of ground-state hydrogen atoms produced by a ring discharge or thermal dissociation,⁹ with an accuracy of a factor of three claimed. Absorption in the H-atom continuum (at 89.0 nm) has been used to measure the H-atom density in a highly ionized discharge.¹⁰ This method is usable only if the line density Π ($= \int_{\text{path}} n(l) dl$, where n is number density) is larger than $\sim 10^{16} \text{ cm}^{-2}$, because of the small cross section; also, this method cannot determine atom

temperature. The latter two experiments both used intense pulsed electric discharges as a source of broadband light which was subsequently narrowed in bandwidth using a monochromator, and neither was able to measure the atom temperature. With the advent of narrow-band tunable vacuum ultraviolet (VUV), laser-induced fluorescence (LIF) on ground-state hydrogen atoms becomes possible. LIF has been used to measure the H-atom density (with Lyman-alpha) in a tokamak,^{11,12} in a glow discharge, and in an atomic gas produced by thermal dissociation.¹³ LIF has also been used to directly determine the density of H-atoms in the $n=2$ state using Balmer-alpha radiation,^{14,15} which can be related to the ground-state density by means of a model.¹⁶ However, accurate modeling of relative ground- and excited-state populations is difficult for low electron temperatures (e.g. 2 eV) and non-Maxwellian electron energy distribution functions (EEDF's) typical of ion-sources because many parameters are not well-known such as wall reaction coefficients and the EEDF.

Absorption at discrete transitions provides another means to measure atom density and temperature. Measurement of absolute photon flux is not required, and the oscillator strengths of the transitions involved are well known,¹⁷ which allows for determination of absolute concentration. LIF allows spatial profiles of concentrations to be determined, but absorption, while useful only for measuring line densities, can be made much less susceptible to background signal (from plasma-produced photons collected at the detectors). Absorption also requires less extensive optical access to the plasma, as there is no need for large-solid-angle collection optics. Measuring the ground-state hydrogen atom population directly requires Lyman-series radiation, which is in the VUV. Narrow-band tunable VUV is generally available only through non-linear processes in gases, of which the most commonly used is four-wave mixing.

Resonant four-wave sum-frequency mixing (FWSM) is a method of VUV production which has been reported for generation of frequencies including the Lyman series in

atomic hydrogen.¹⁸⁻²⁰ It allows production of large VUV fluxes without phase-matching, and it produces VUV over a wide continuous range of frequencies by changing the frequency of only one of the lasers. A review of the principles and applications of FWSM has been recently published.²¹ Briefly, FWSM is a coherent process in which a non-linear medium, mercury vapor in this application, is exposed to intense electric fields of (angular) frequencies ω_1 and ω_2 , and converts some of the energy from those fields into radiation at $2\omega_1 + \omega_2$. By choosing $2\omega_1$ to correspond to the energy difference of the ground-state and an excited-state of the medium of the same parity, this process is made resonant. The intense electric fields generally require high-power pulsed lasers. Fig. 1 schematically illustrates the process of FWSM, specific to the present application.

This paper describes a VUV laser-spectrometer system which is used to measure the line density of ground-state hydrogen atoms in a hydrogen discharge of high background VUV flux, using Lyman-beta or Lyman-gamma radiation generated by FWSM in mercury vapor.

II. EXPERIMENTAL METHOD

A schematic of the experimental apparatus is shown in Fig. 2. An excimer laser pumps two dye lasers, which generate the ω_1 and ω_2 beams. These beams are merged in a prism, and are focussed by an achromatic lens into a mercury vapor cell, where the VUV is generated coincident with the original beams. Two stages of differential pumping immediately follow. All three beams are then incident upon a grating which disperses them. The first order VUV beam, the probe beam, is directed towards the plasma of interest, while the second order VUV beam, the normalization beam, is directed onto a detector. Light of all other wavelengths is discarded at this point. After passing through the plasma chamber, which is differentially pumped, the

probe beam enters a monochromator which is tuned to allow full transmission of the beam, while rejecting most of the background photon flux from the plasma. Another detector is mounted on the output side of the monochromator.

The pump laser is a XeCl excimer laser (Lambda Physik EMG201E) pulsed at 10 Hz. Each pulse provides approximately 450 mJ at 308 nm in 20 ns. The pump beam is directed into two dye lasers (Lambda Physik FL2002E) using a 50-50 beam splitter. The ω_1 dye laser generates approximately 25 mJ of 538 nm light (Coumarin 540A dye). An intracavity etalon reduces the linewidth to 0.04-0.05 cm^{-1} , and a KDP crystal is used to double the frequency of the emitted light, yielding ~3 mJ at 269 nm, which is tuned to correspond to one half of the $(6s8s) \ ^1S_0$ energy level in mercury. This energy level has been shown to be efficient for VUV production in the range of Lyman-beta (102.6 nm) and Lyman-gamma (97.2 nm).⁸ Frequency calibration is performed by observing fluorescence of I_2 vapor produced by the fundamental beam.²² The accuracy of the calibration is estimated to be +/- 0.02 cm^{-1} for the frequency-doubled light. The ω_2 dye laser generates ~15 mJ of 433 nm light for Lyman-beta production (Coumarin 440 dye), or 351 nm for Lyman-gamma production (DMQ dye). The bandwidth is nominally 0.20 cm^{-1} . The tuning calibration of this laser is performed indirectly by observing absorption of generated VUV in krypton, xenon, or H_2 at known frequencies. The beams from each laser are directed to a calcite Glan-Taylor prism which merges the two beams. The beam paths have been chosen so that the beams are coincident in time, and the various prisms are adjusted to make the two beams spatially coincident. The final alignment is done by optimizing the VUV output.

The two dye laser beams are focussed by a 25-cm focal length quartz achromatic lens into the mercury-vapor cell, shown separately in Fig. 3, where the VUV is generated colinearly with the original laser beams. The design of the cell is loosely based on heat pipe technology.²³ The cell is nickel plated on the inside to avoid

chemical reactions. The input window is a piece of Suprasil quartz plate. A 0.025-mm thick stainless steel foil is mounted on the exit arm, through which the lasers burn a hole in a few minutes, forming a tight differential pumping constriction ($\sim 0.20 \text{ mm}^2$) that is automatically aligned with the beams. The bottom arm of the cell contains heated liquid mercury maintained at a well defined temperature by a copper jacket. Typical operating temperature of the jacket is $230 \text{ }^\circ\text{C}$, which corresponds to an equilibrium mercury vapor pressure of 43 torr; however, since the wall surfaces near the mixing region are much cooler than the reservoir, we expect that the actual pressure in the mixing region is considerably less than this. Helium, typically at a pressure of 30 torr, is used as a buffer gas to help confine the mercury vapor. The helium inlet location and the restrictor discs are chosen so as to minimize flow and turbulence in the cell. A capacitance manometer is connected to the top arm of the cell to measure the pressure. Water cooling lines are wrapped around the upper and side arms adjacent to the intersection region in order to condense mercury before it travels an appreciable distance. Liquid nitrogen cooling lines on the input arm serve to prevent mercury vapor from condensing on the inside of the input window. Two stages of differential pumping immediately follow the cell. The first stage is evacuated by a mechanical pump with an effective pumping speed of a few liters/sec, and has a pressure of ~ 1.0 torr. The second stage is pumped by a turbo-pump with a pumping speed of approximately 100 liters/sec. The pressure in the second stage is ~ 1 mtorr.

The beam passes through another differential pumping aperture into a 35-cm diameter chamber (the "grating chamber") which contains a blazed grating (Milton Roy, 2400 grooves/mm, blaze angle 5.5° , radius of curvature 100 cm), a two-stage chevron microchannel plate (MCP) detector (varian 8946ES plates), and a photodiode sensitive to the visible and near UV. The chamber is pumped by a liquid nitrogen trapped diffusion pump, with an effective pumping speed of 600 liters/sec. The photodiode is used to check system alignment by collecting stray light from the grating

when the system is under vacuum. The grating is mounted in a two-axis tilter which is controlled by two externally-mounted micrometers. The probe beam is refocussed by the grating and is directed 45° from the incident beam through the plasma chamber. The normalization beam detector is positioned to intercept the normalization beam from the grating. A series of biased shields prevents signals caused by charged particles impinging upon the detector. Background signal from this detector, caused by stray light of other wavelengths, is negligible ($< 0.1\%$) compared to the primary signal.

The probe beam passes through the plasma into the vacuum monochromator (Acton VM502, 0.2m), which has its entrance slits at the horizontal focal point of the probe beam. Two collimating discs slightly larger than the beam size are placed on each side of the plasma chamber in order to reduce background photon flux and to allow differential pumping of the plasma source. The monochromator slits are adjusted so that the full beam passes through without attenuation. The probe beam detector, which is similar in construction to the normalization beam detector, is attached to the output side of the monochromator. The frequency resolution of the system is controlled by the narrow VUV bandwidth, not by the monochromator, which acts simply as a narrow-band filter to increase the signal-to-noise ratio.

The signal from each MCP detector is sent to a charge-sensitive amplifier with a 20 μs decay time, and is sampled with a gated integrator (Stanford Research Systems SR250) using a 3 μs window and a 1 μs delay. These values were chosen empirically so as to minimize background signal caused by the unavoidable electronic noise generated by the firing of the excimer laser. The linearity of both detectors was verified using screens of known transmission, and the proportionality of the two signals was verified. The integrator output signals are collected by a computer while scanning the frequency of the ω_2 laser, which frequency scans the VUV radiation, first with the plasma on and then with the plasma off. Typically data from 100 laser pulses are

recorded for each of ~50 scan points. The spacing of scan points is usually 0.32 cm^{-1} . The data recorded between laser pulses is used to remove baseline drift of the integrators.

The estimated VUV flux is about 10^9 photons/pulse. The estimate was made by comparing the average single photon signal with the full pulse and scaling by the estimated efficiencies of the gratings and detectors.

To determine the VUV bandwidth, an absorption profile of Kr was measured. The absorption profile of the krypton line at 103.0023 nm (Fig. 4) has an observed width of 0.30 cm^{-1} . Krypton has a doppler width of 0.13 cm^{-1} at room temperature. Assuming the linewidth and the laser bandwidth add in quadrature, we obtain 0.27 cm^{-1} (FWHM) for the VUV bandwidth.

It should be mentioned that the lasers are not completely spectrally pure, which causes the VUV to be spectrally impure also. The fraction of impurity radiation which reaches the primary detector, designated the leakage fraction, is important since this fraction will determine the maximum true attenuation that can be measured. This fraction was reduced, as will be described in section IV, to $<0.5\%$.

III. A SAMPLE MEASUREMENT

As an example of the use of the spectrometer system, measurements have been made of the hydrogen atom density in discharges in a multi-cusp negative-ion-source. The transmission of the plasma for the VUV probe beam is measured as a function of wavelength in the neighborhood of the appropriate transition by measuring the (normalized) signal from the primary detector with and without discharge, from which the integrated absorbance A can be calculated:

$$A = \int \ln [I_{\text{off}}(\lambda) / I_{\text{on}}(\lambda)] d\lambda, \quad (1)$$

where $I(\lambda)$ is the probe beam signal divided by the normalization beam signal. The subscripts refer to the discharge status. The integrated absorbance is proportional to the line density, regardless of the shape of the transition lineshape, for a perfectly monochromatic probe beam. The proportionality factor Σ is the integral of the cross section over wavelength in the region of the resonance, which can be written either in terms of the Einstein A coefficient (the $nP \rightarrow 1S$ decay rate),

$$\Sigma = 3\gamma\lambda_0^4 / 8\pi c, \quad (2)$$

or the oscillator strength:

$$\Sigma = \pi f r_e \lambda_0^2, \quad (3)$$

where γ is the decay rate of the nP state (n is the principal quantum number), λ_0 is the wavelength of the transition, c is speed of light, f is the oscillator strength, and r_e is the classical electron radius. It should be noted that the oscillator strength is assumed to already have the degeneracy ratio factor included in it, which is $3/1 = 3$ for $1S \rightarrow nP$ transitions. The line density, $\Pi = nI$ (n = average atom density, I = path length), is then:

$$\Pi = A / \Sigma \quad (4)$$

A plot of absorbance vs wave number is shown in Fig. 5 for the H-atom transition $1S \rightarrow 3P$ (Lyman-beta) for typical discharge parameters in a large multi-cusp experimental negative-ion source. In this instance the measured H-atom line density is $8.21 \cdot 10^{13} \text{ cm}^{-2}$, with an error of ~4%, as discussed in section IV. The path length

in the source is 31 cm, leading to an average number density of $2.65 \cdot 10^{12} \text{ cm}^{-3}$. The atom temperature ($2/3$ of average kinetic energy, assuming isotropy), as determined by least-squares same-area Gaussian fit, is measured to be 0.058 eV in this discharge, and is estimated to be accurate to within 10%. We have recently made further measurements of H-atom density using Lyman-gamma radiation, which increases the maximum observable line density by a factor of 3.

IV. DISCUSSION

The statistical error is less than 2% for the line density measurement. The systematic error of the line density measurement depends on three factors: the ratio of the transition linewidth to the probe bandwidth, the maximum true absorbance, and the anomalous VUV leakage fraction discussed previously. The latter factor is the one most difficult to estimate accurately. This undesired radiation will not be absorbed by the hydrogen atoms to the same extent as radiation within the central line, which causes a large error in the attenuation measurement when the attenuation is large. The error introduced determines the maximum true attenuation that can be measured accurately. To reduce the spectral impurities, a VUV absorption spectrum is measured for a transition which should be optically opaque at line center ($I_{\text{transmitted}} / I_{\text{incident}} < 10^{-4}$). With this attenuation, any residual transmission at line center is due to spectral impurities. The alignment of the laser optics is then adjusted to minimize this transmission. A D_2 line was selected [B - X (8,0) P(6), at $96,664.5 \text{ cm}^{-1}$],²⁴ as its linewidth (0.62 cm^{-1} FWHM) is wide enough to completely absorb the desired VUV line but narrow enough to give high sensitivity to spectral impurities. At optimum alignment, the fraction transmitted is 0.2-0.3%.

Neglecting the leakage fraction, the fractional error in the measured absorbance

caused by the finite bandwidth of the probe beam can be shown to be proportional to the product of the oscillator strength and the square of the VUV bandwidth (see Appendix for details) for a VUV line shape that is Gaussian, and a bandwidth that is small compared to the transition linewidth. This implies that to minimize this error, the VUV bandwidth should be small, and the absorbance should be small.

Numerical analyses were performed to determine the error in the measured line density as a function of the bandwidth ratio, the leakage fraction, and the maximum absorbance. The transition lineshape was assumed to be Gaussian. The probe beam spectral profile was also assumed to be Gaussian, except for the leakage factor, given as a parameter, which was assumed to be so far off center as to be unattenuated. The error is always such as to underestimate the true line density. For the measurement of section III, where the bandwidth ratio was ~ 7 , the maximum absorbance was 3.5, and the leakage factor was assumed to be $\sim 0.5\%$, the line density error was 4%, and was mostly due to the leakage factor, not the bandwidth ratio, which would have given an error of $\sim 1.3\%$ by itself. A study of the error produced by different parameters indicated that the primary source of error in our parameter regime is the fact that the leakage factor is not small compared to the maximum true attenuation.

Steering of the beam by a non-uniform plasma could cause an error in the measurement. A simple calculation was performed to determine the maximum deflection of the beam at the monochromator input slits that could be expected due to a transverse gradient in the atom density (and therefore index of refraction), and it was found that the deflection is very small compared to the slit size. This is to be expected, since the real part of the dielectric function has a maximum amplitude of the order of the wavelength (~ 100 nm) divided by the $1/e$ length (~ 10 cm), or 10^{-6} . It is noted here also that no off-resonance continuum absorption is observed with the discharge on.

The measurable density range of the system depends on the atom temperature. For an atom temperature of 0.1 eV, which is fairly typical of medium-power plasmas, and for peak absorbances between 0.05 and 4, line densities from $2 \cdot 10^{12} \text{ cm}^{-2}$ (using Lyman-beta) to $4 \cdot 10^{14} \text{ cm}^{-2}$ (using Lyman-gamma) can be measured. The bandwidth of the generated VUV corresponds to a H-atom temperature of $\sim 15 \text{ }^\circ\text{K}$, so any temperature that can be reasonable expected in a plasma can be measured (although at high absorbance and low atom temperature the errors become larger).

It should be noted that this system could be used to measure the density of any species that has a known oscillator strength in the frequency range of this system, and which satisfies the above criteria on absorbance. The tuning range of the VUV extends from 87,000 to 103,500 cm^{-1} using the (6s8s) $^1\text{S}_0$ state, if the ω_2 laser is restricted to operation without a frequency-doubling crystal. By simply tuning the ω_1 laser to one half of the (6s7s) $^1\text{S}_0$ energy level, the lower limit is extended to $\sim 82,000 \text{ cm}^{-1}$, which would include Lyman-alpha. Below $\sim 82,000 \text{ cm}^{-1}$ the third-order susceptibility shows more severe variations.²⁰ Higher frequencies are available (at reduced flux) by employing the (6s7d) $^3\text{D}_2$ state as the resonant state, which would increase the upper limit to 106,200 cm^{-1} . It is also possible to operate the ω_2 laser with a frequency-doubling crystal, which extends the VUV upper limit to $\sim 80 \text{ nm}$.¹⁸ By using Lyman-alpha, measurement of H-atom densities a factor of six smaller than those measured with Lyman-beta could be achieved. This transition has the largest oscillator strength in the Lyman series. If Lyman-delta or higher-order Lyman lines are produced, the measurable density limit will increase, since the oscillator strengths of the (nP) \rightarrow (1S) transitions decrease as n^{-3} .¹⁷

CONCLUSION

We have described a VUV laser-spectrometer which is used to measure the line density and temperature of ground-state hydrogen atoms in a plasma by absorption of narrow-band Lyman-beta or Lyman-gamma radiation, which is generated by resonant four-wave sum-frequency mixing in mercury vapor. Measurements are possible even for room temperature atoms. The accuracy of the line-density measurement is estimated to be ~4%. For an atom temperature of 0.1 eV, line densities of $2 \cdot 10^{12} \text{ cm}^{-2}$ to $4 \cdot 10^{14} \text{ cm}^{-2}$ can be measured. By a modest extension, the lower limit can be reduced to $3 \cdot 10^{11} \text{ cm}^{-2}$. Because this system permits generation of VUV over a wide continuous frequency range (~82,000 to 106,200 cm^{-1}), it could also be used to measure line densities of other species that have optical densities in the proper range.

APPENDIX

It is shown that the relative error ϵ in measuring the absorbance of a medium at a given frequency, due to the finite bandwidth of the probe beam, is proportional to the square of the bandwidth of the probe beam, the square of the slope of the true absorbance with respect to ω (angular frequency), and to the inverse of the true absorbance. It is assumed that the probe beam is Gaussian in frequency space, that the absorbance can be represented by a linear function over the width of the probe beam, and that the error itself is small compared to unity. The probe beam spectral profile, normalized to 1, is given by

$$f(\omega) = [(\pi)^{0.5}(\omega_d)]^{-1} \exp\{-[(\omega-\omega_0)/\omega_d]^2\} \quad (5)$$

where ω_0 is the center frequency and ω_d is the 1/e half-width of the probe beam. The absorbance can be represented (for fixed ω_0) as

$$A(\omega) = a(\omega-\omega_0)+b \quad (6)$$

where a and b are constants. Then the fraction of the probe beam that is transmitted, T , is given by the convolution integral

$$T = \int f(\omega) \exp[-A(\omega)] d\omega \quad (7)$$

This can be easily evaluated, yielding

$$T = \exp(-b) \cdot \exp[(a\omega_d/2)^2]. \quad (8)$$

The first factor is clearly what one obtains for a perfectly monochromatic beam. The second factor is the error factor, which goes to one as ω_d goes to zero, as expected. Note the error is always greater than one, leading to less measured attenuation. For our data the exponent in the second term is small and thus one obtains for the relative error of the absorbance

$$\varepsilon = (a\omega_d/2)^2/b, \quad (9)$$

which scales as the square of the width of the probe beam, the square of the slope of true absorbance with respect to ω , and inversely with the true absorbance as

previously stated. Therefore, the relative error in the measured absorbance is proportional to the corresponding oscillator strength and to the square of the probe beam bandwidth, because, for a given atom velocity distribution, the true absorbance in the neighborhood of a transition is proportional to the oscillator strength. The relative error in the integral of the measured absorbance clearly has these same scaling properties.

ACKNOWLEDGEMENTS

The authors would like to thank Drs. W. G. Graham, P. Gohil, and E. M. Bernstein for their contributions during the early part of this work. We would also like to thank Dr. J. W. Hepburn for his assistance in the implementation of sum-frequency generation of VUV radiation. This work was supported by Los Alamos National Laboratory, the Air Force Office for Scientific Research, and the U.S. Department of Energy under contract No. DE-AC03-76SF00098.

a) also associated with Department of Physics, University of California, Berkeley,
CA 94720

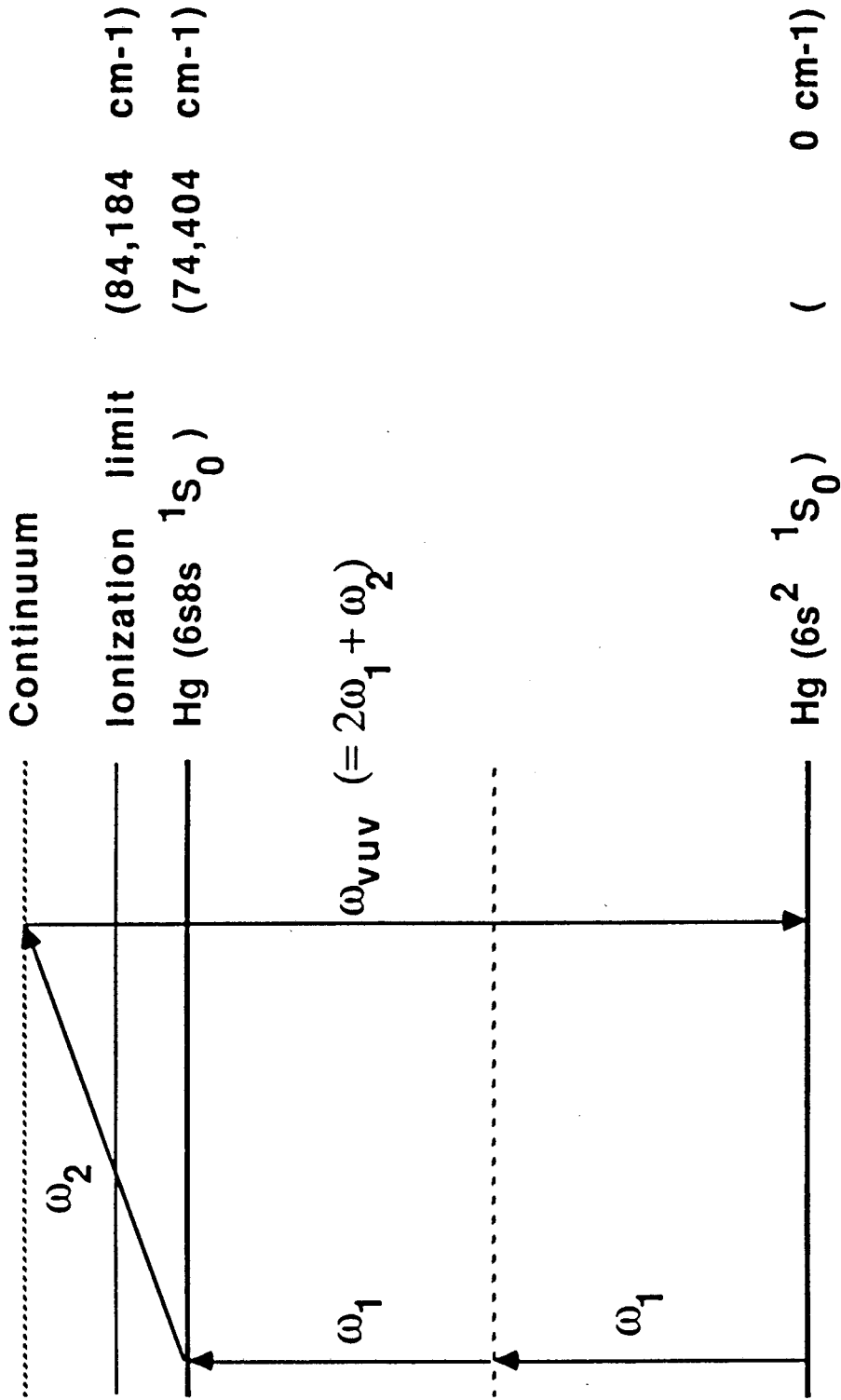
REFERENCES

1. M. Bacal, A. M. Bruneteau, W. G. Graham, G. W. Hamilton, and M. Nachman, J. Appl. Phys. 52, 1247 (1981).
2. K. N. Leung and W. B. Kunkel, Phys. Rev. Lett. 59, 787 (1987).
3. For a discussion and further references, see J. R. Hiskes and A. M. Karo, J. Appl. Phys. 56, 1927 (1984).
4. R. I. Hall, I. Cadez, M. Landau, F. Pichou, and C. Schermann, in Proceedings of IAEA Technical Meeting on Negative Ion Beam Heating, Culham Laboratory, England, July 15-17, 1987.
5. V. G. Dudnikov, Proc. IV All-Union Conf. on Charged Particle Accelerators, Moscow, 1974, Nauka 1975 Vol. 1, p. 323.
6. G. E. Derevyankin and V. G. Dudnikov, in Production and Neutralization of Negative Ions and Beams, edited by K. Prelec (American Institute of Physics, New York, 1984), p. 376.
7. M. Bacal, in Production of Negative Ions and Beams, edited by J. G. Allesi (American Institute of Physics, New York, 1987), p. 120.
8. H. Suzuki and K. Nobata, Jpn. J. Appl. Phys. 25, 1589 (1986).
9. P. Bogen and Y. T. Lie, Appl. Phys. 16, 139 (1978).
10. P. R. Forman and W. B. Kunkel, Phys. Fluids 11, 1528 (1968).
11. R. W. Dreyfus, P. Bogen, and H. Langer, in Laser Techniques for Extreme Ultraviolet Spectroscopy, edited by I. J. McIlrath and R. R. Freeman (American Institute of Physics, New York, 1982), p. 57.
12. T. Kajaiwara, M. Inoue, T. Okada, K. Muraoka, M. Akazaki and M. Maeda, Rev. Sci. Instrum. 56, 2213 (1985).
13. P. Mertens and P. Bogen, Appl. Phys. A 43, 197 (1987).

14. D. Okano, K. Uchino, A. Shimizu, K. Muraoka, M. Maeda, M. Akazaki, S. Sudo, O. Motojima, A. Iiyoshi, and K. Uo, *J. Nucl. Mater.* 147, 504 (1987).
15. M. Nightingale, A. Holmes, M. Forrest, and D. Burgess, *J. Phys. D* 19, 1707 (1986).
16. P. Gohil and D. Burgess, *Plasma Phys.* 25, 1149 (1983).
17. H. A. Bethe and E. E. Salpeter, Quantum Mechanics of One- and Two-Electron Atoms (Plenum, New York, 1957).
18. P. R. Herman and B. P. Stoicheff, *Opt. Lett.* 10, 502 (1985).
19. R. Hilbig and R. Wallenstein, *IEEE J. Quantum Electron.* QE-19, 1759 (1983).
20. F. S. Tomkins and R. Mahon, *Opt. Lett.* Z, 304 (1982).
21. C. R. Vidal, in Topics in Applied Physics. Volume 59: Tunable Lasers, edited by L. F. Mallenauer and J. C. White (Springer-Verlag, Berlin, 1987), p. 57.
22. S. Gerstenkorn and P. Luc, Atlas du Spectre D'Absorbtion de la Molecule D'Iode (Editions du Centre National de la Recherche Scientifique, Paris, 1978).
23. C. R. Vidal and J. Cooper, *J. Appl. Phys.* 40, 3370 (1969).
24. I. Dabrowski and G. Herzberg, *Can. J. Phys.* 52, 1110 (1974).

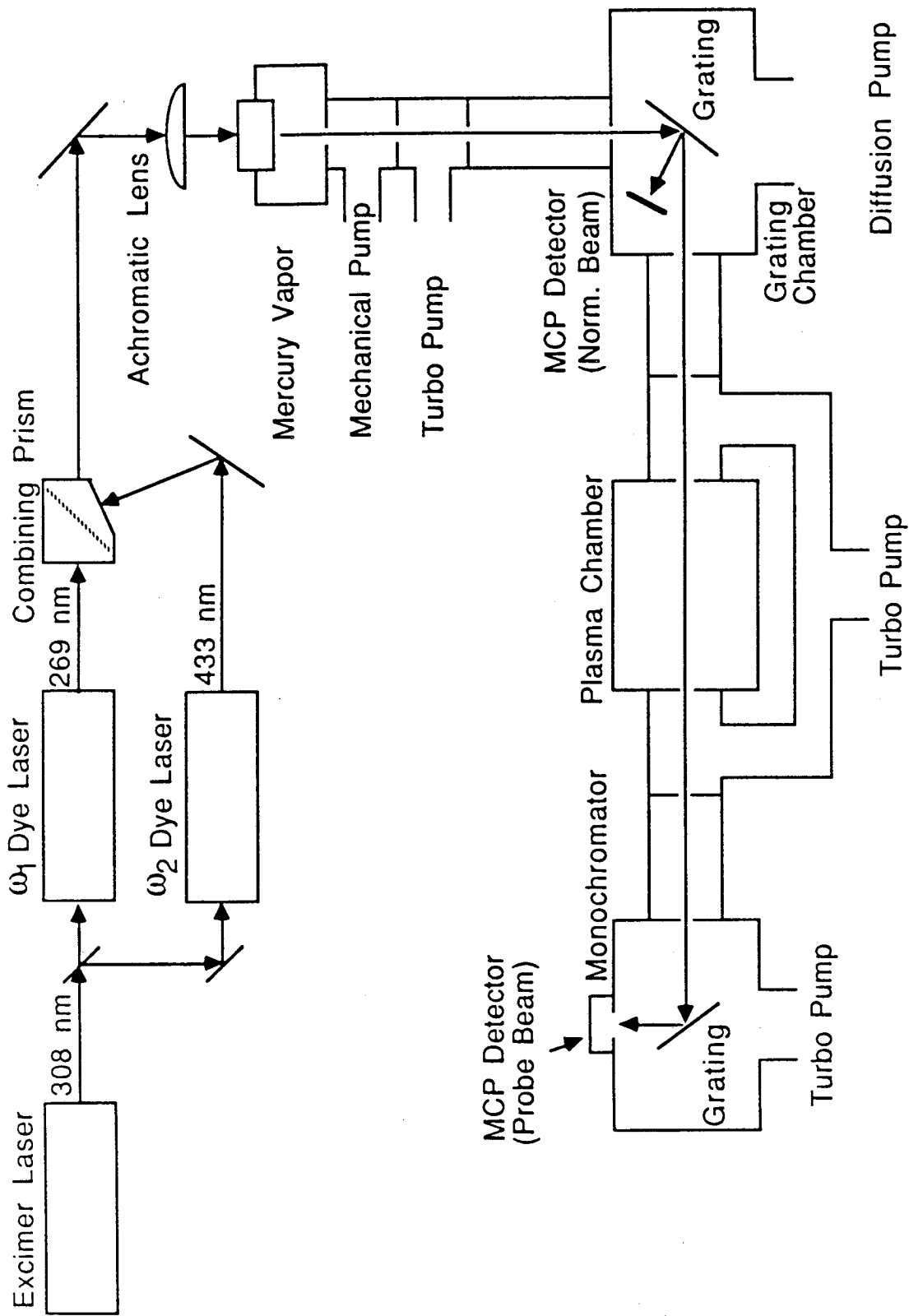
Figure Captions

- Fig. 1 Schematic illustration of resonant four-wave sum-frequency mixing, specific to present work.
- Fig. 2 Block diagram of VUV absorption-spectrometer system. The VUV beam is generated by four-wave mixing in a mercury-vapor cell.
- Fig. 3 Schematic of mercury-vapor cell used for VUV generation (not to scale). Inside diameter of horizontal arms is 10 mm, horizontal length is 15 cm.
- Fig. 4 VUV absorption profile in $3 \cdot 10^{-5}$ Torr of Kr gas at 300 °K (no discharge), used for VUV bandwidth determination. Measured linewidth is 0.30 cm^{-1} , yielding a VUV bandwidth of 0.27 cm^{-1} , assuming quadrature summing of widths. Spacing of points is 0.032 cm^{-1} . Statistical error bars are less than 0.01.
- Fig. 5 VUV absorption profile showing attenuation by hydrogen atoms, measured during a discharge, using Lyman-beta radiation. Measured line density and temperature are $8.2 \cdot 10^{13} \text{ cm}^{-2}$ and 0.058 eV respectively. H_2 pressure was $7 \cdot 10^{-4}$ Torr. Arc parameters were 8 A at 100 V, in a multicusp chamber of volume 6.5 liters. Statistical error bars not visible this scale.



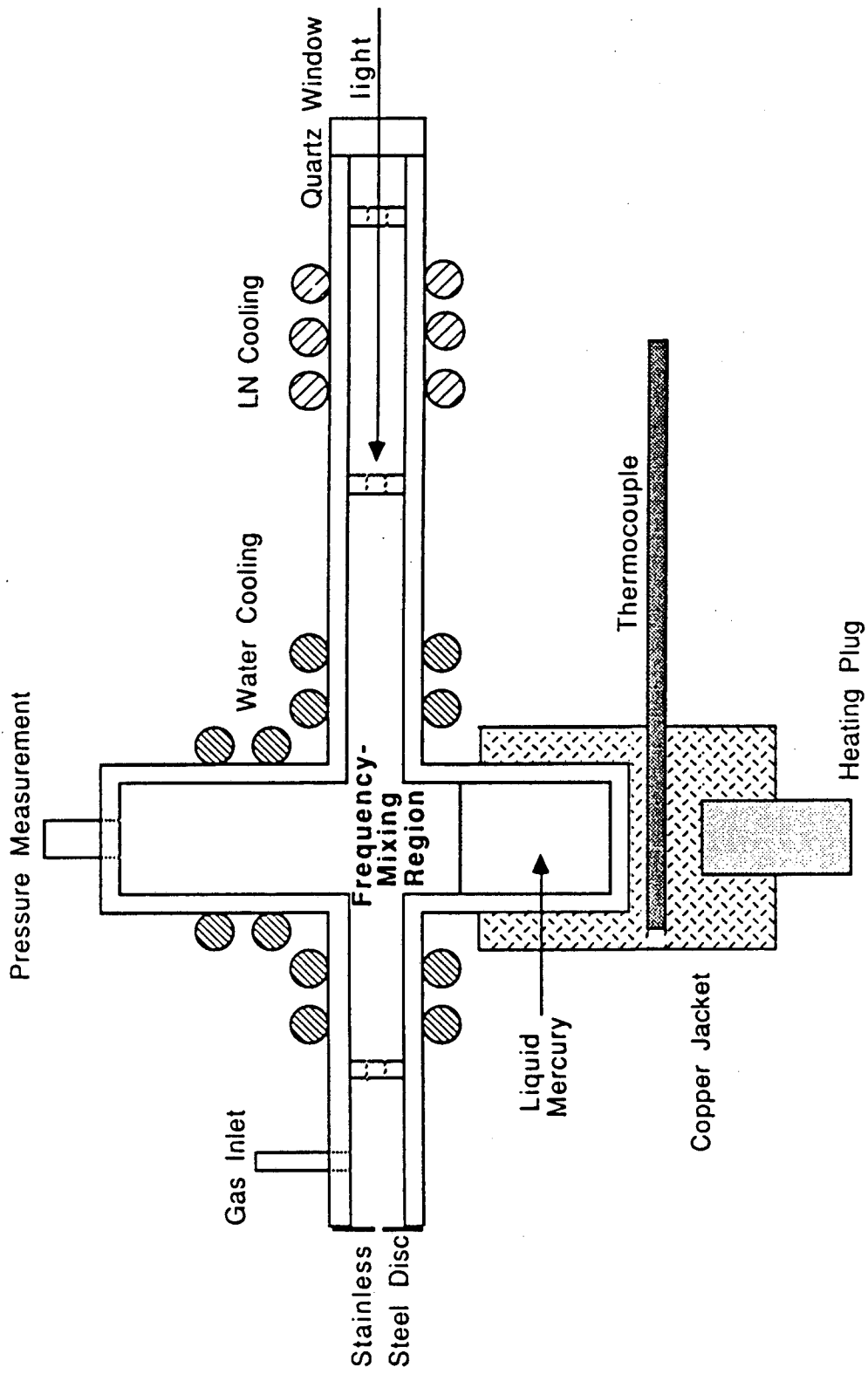
XBL 882-451

Figure 1



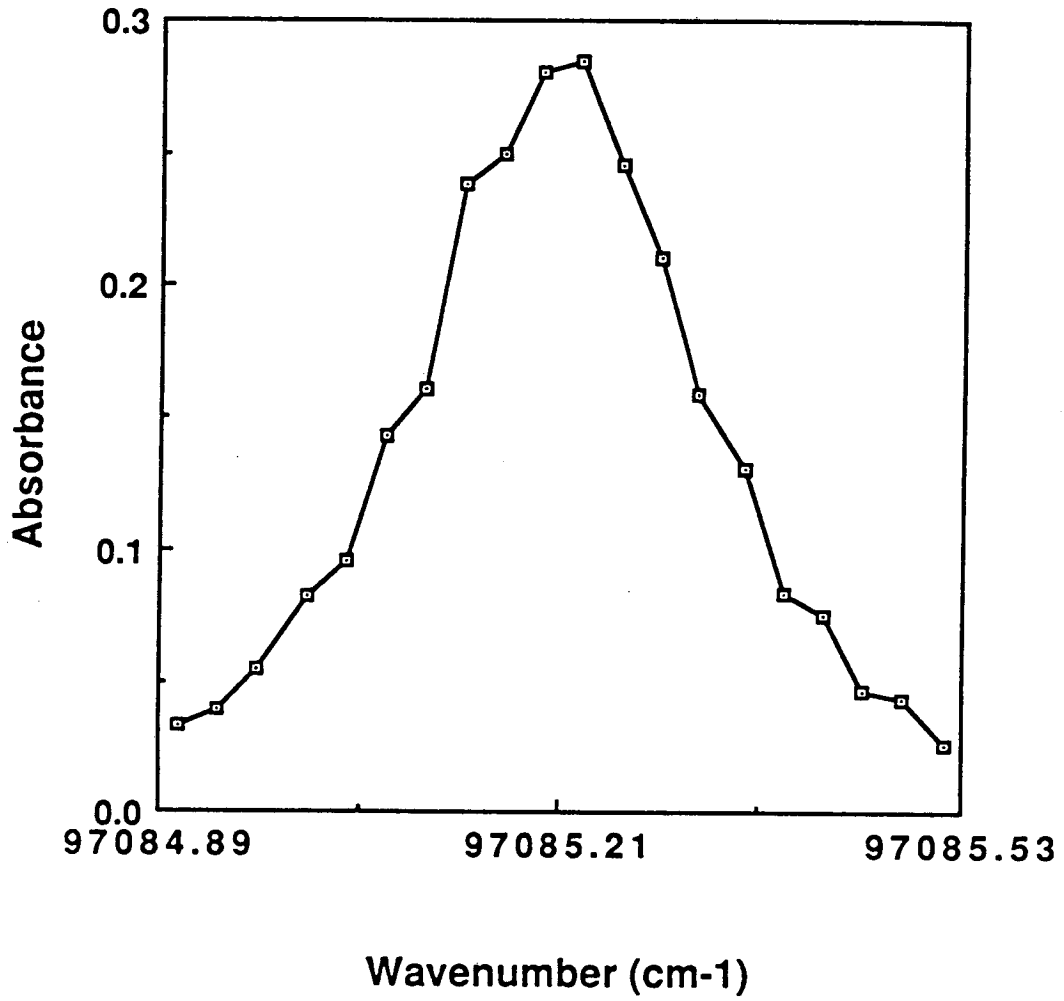
XBL 882-452

Figure 2



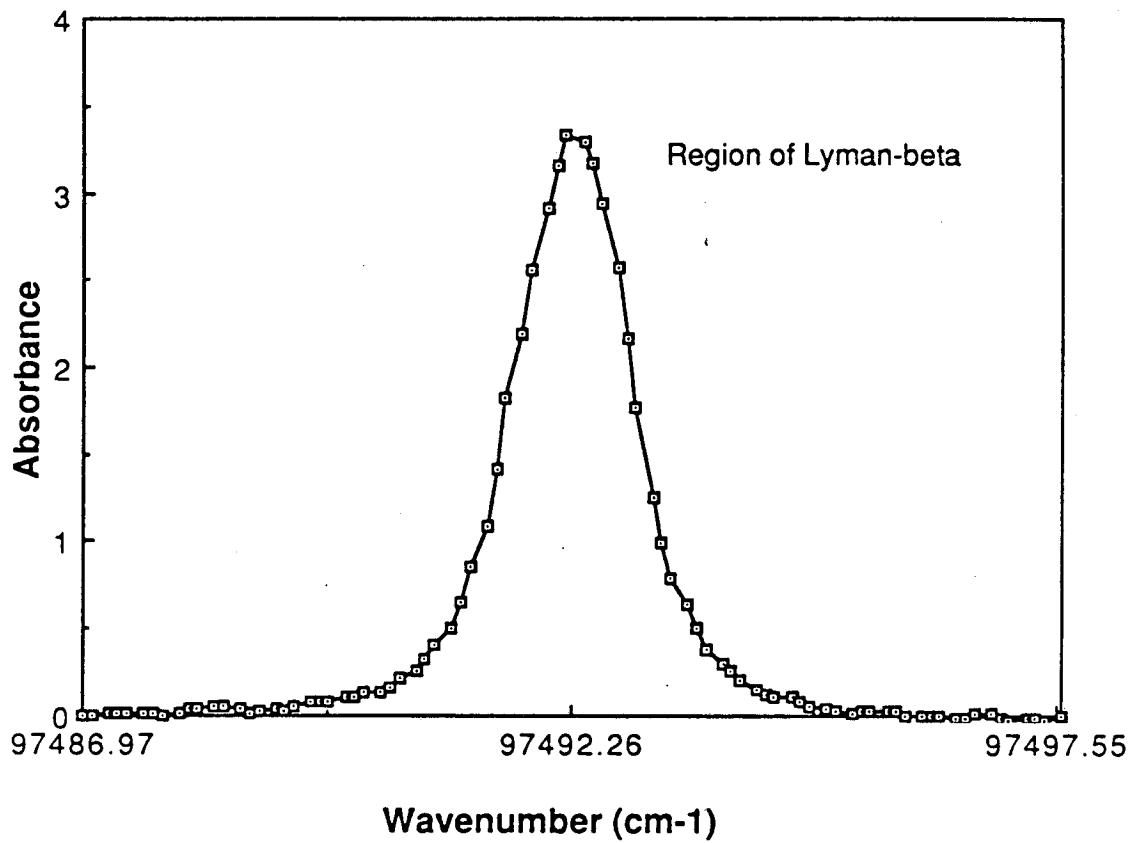
XBL 882-448

Figure 3



XBL 882-449

Figure 4



XBL 882-450

Figure 5

LAWRENCE BERKELEY LABORATORY
TECHNICAL INFORMATION DEPARTMENT
UNIVERSITY OF CALIFORNIA
BERKELEY, CALIFORNIA 94720